Pharm Res (2014) 31:2367–2382
DOI 10.1007/s11095-014-1333-3

RESEARCH PAPER

Reduced Physiologically-Based Pharmacokinetic Model of Repaglinide: Impact of OATP1B1 and CYP2C8 Genotype and Source of In Vitro Data on the Prediction of Drug-Drug Interaction Risk

Michael Gertz • Nikolaos Tsamandouras • Carolina Säll • J. Brian Houston • Aleksandra Galetin

Received: 20 October 2013 / Accepted: 8 February 2014 / Published online: 13 March 2014

ABSTRACT

Purpose To investigate the effect of OATP1B1 genotype as a covariate on repaglinide pharmacokinetics and drug-drug interaction (DDIs) risk using a reduced physiologically-based pharmacokinetic (PBPK) model.

Methods Twenty nine mean plasma concentration-time profiles for *SLCO1B1* c.521T>C were used to estimate hepatic uptake clearance (CL_{uptake}) in different genotype groups applying a population approach in NONMEM v.7.2.

Results Estimated repaglinide CL_{uptake} corresponded to 217 and 113 μL/min/10^6 cells for *SLCO1B1* c.521TT/TC and CC, respectively. A significant effect of OATP1B1 genotype was seen on CL_{uptake} (48% reduction for CC relative to wild type). Sensitivity analysis highlighted the impact of CL_{met} and CL_{diff} uncertainty on the CL_{uptake} optimization using plasma data. Propagation of this uncertainty had a marginal effect on the prediction of repaglinide OATP1B1-mediated DDI with cyclosporine; however, sensitivity of the predicted magnitude of repaglinide metabolic DDI was high. In addition, the reduced PBPK model was used to assess the effect of both CYP2C8*3 and *SLCO1B1* c.521T>C on repaglinide exposure by simulations; power calculations were performed to guide prospective DDI and pharmacogenetic studies.

Conclusions The application of reduced PBPK model for parameter optimization and limitations of this process associated with the use of plasma rather than tissue profiles are illustrated.

KEY WORDS drug-drug interactions · OATP1B1 · physiologically-based pharmacokinetic models · repaglinide

INTRODUCTION

Physiologically-based pharmacokinetic (PBPK) modeling is increasingly used as a decision-making tool in different phases of drug development (1,2). In particular it is becoming important for the prediction of enzyme-transporter-mediated pharmacokinetics and associated complex drug-drug interactions (DDIs) (3–6). A number of recent studies have integrated transporter kinetic data (e.g., scaled active uptake clearance and/or biliary efflux), together with passive permeability (CL_{diff}), metabolic clearance (CL_{met}) and intracellular binding within the whole body PBPK model framework (4,7–11). In all these cases, permeability limited principles were applied for the liver model, either by introducing separate liver tissue and blood compartments (8) or by subdividing liver into multiple units of extracellular and intracellular compartments connected by blood flow (7,9); the kinetics of other organs in the PBPK model were generally described as perfusion rate limited.

It is evident that the methods used to generate transporter *in vitro* kinetic data vary substantially across studies (6). In some instances, mechanistic 2- or 3-compartment models including media, cellular and bile compartments were applied for the characterization of transporter substrates *in vitro* (12–18). These mechanistic *in vitro* models allowed simultaneous characterization of multiple processes in hepatocytes, generating parameter estimates compatible for subsequent PBPK modeling (7,12,15). Alternatively, studies have used metabolic and

Electronic supplementary material The online version of this article (doi:10.1007/s11095-014-1333-3) contains supplementary material, which is available to authorized users.

M. Gertz • N. Tsamandouras • C. Säll • J. B. Houston • A. Galetin (✉)
Centre for Applied Pharmacokinetic Research
Manchester Pharmacy School
The University of Manchester, Oxford Road
M13 9PT Manchester, UK
e-mail: Aleksandra.Galetin@manchester.ac.uk

Present Address:
M. Gertz
F. Hoffmann-La Roche, Modelling and Simulation Pharmaceutical Sciences
pRED, Basel, Switzerland

transport kinetic data generated in different *in vitro* systems (5,19); scaling of each parameter was done according to the *in vitro* system used and integration of these data was performed using permeability liver models.

Direct use of *in vitro* uptake transporter kinetic data in either static or PBPK models has resulted in on average 17- to 58-fold under-prediction of hepatic clearance for the comparable drug set. This trend was apparent regardless of the cellular source of *in vitro* transporter data (plated, in suspension or sandwich cultured hepatocytes) (6,7,14) and is analogous to under-prediction reported previously for predominantly metabolized drugs (20). Loss or reduction in OATP activity/expression due to hepatocyte isolation, cryopreservation, increased culturing time and discrepancy in transporter expression in hepatocytes relative to the intact tissue (21–25) may all contribute to differences in the transporter activity and in some cases large extent of under-prediction observed. To bridge the gap in transporter *in vitro-in vivo* extrapolation, clinical plasma concentration-time data have been increasingly used to optimize active uptake parameters (either CL_{uptake} or uptake V_{max}) in PBPK models (4,5,7–9). The rationale behind this approach is that the active uptake is a major contributor to the hepatic clearance of the drugs investigated and therefore assumed to account for the magnitude of the under-prediction observed. The optimization process is generally performed by fixing the remaining model parameters (e.g., CL_{met} or CL_{diff}) and by not accounting for their uncertainty (26).

Repaglinide represents an interesting example of a drug with a complex disposition scheme considering its active uptake, relatively high passive diffusion into hepatocytes and multiple metabolic pathways (15,27). In addition, up to 11- and 17-fold range in repaglinide C_{max} and AUC has been reported following a standard 0.25 mg dose; this large inter-individual variability is generally associated with polymorphism in the *SLCO1B1* gene encoding for the hepatic uptake transporter OATP1B1 (28). In contrast, CYP2C8*3 polymorphism has been reported to either have no significant effect (29,30) or to moderately (<50%) decrease repaglinide plasma exposure (28,31). The effect of CYP2C8*3 polymorphism is difficult to assess clinically in conjunction with altered OATP1B1 activity. An adequately powered study in terms of sample size is crucial, in particular considering frequency of CYP2C8*3 and OATP1B1 521CC. Most of the reported repaglinide clinical studies so far focus on OATP1B1 polymorphism in isolation and often include non-carriers of CYP2C8*3 allele (32).

Previously, we have successfully applied whole body PBPK model for the prediction of repaglinide DDI with cyclosporine (4). In the current study, we have developed a reduced hybrid repaglinide PBPK model to investigate the effect of OATP1B1 genotype as a covariate on repaglinide pharmacokinetics. Minimal or semi-mechanistic models consider a reduced number of tissue compartments compared to a whole-body PBPK model, while keeping a mechanistic description of metabolism/transporter processes in the organs of interest (e.g., intestine and liver) (33–35). In this study, clinical data for the most prevalent OATP1B1 polymorphism, *SLCO1B1* c.521T>C, were used in the population modeling approach in NONMEM v.7.2 to estimate repaglinide hepatic intrinsic uptake clearance (CL_{uptake}) in different OATP1B1 genotype groups and perform comparison to the reported *in vitro* data (15) for this parameter. The reduced model was used to simulate repaglinide plasma- and liver profiles in different SLCO1B1 population groups. In addition, sensitivity analyses were performed and the impact of applying a range of fixed CL_{met} and CL_{diff} (corresponding to 0.1 to 10-fold of the original parameter value and in agreement with reported values for these parameters in the literature) on the CL_{uptake} optimization was assessed. Subsequently, propagation of the uncertainty in these parameters on the predicted magnitude of repaglinide DDI with either metabolic or inhibitors of hepatic uptake was investigated. Following model validation, the reduced PBPK model was used to predict the impact of the CYP2C8*3 polymorphism on plasma repaglinide exposure and DDI risk, by also taking into account *SLCO1B1* c.521T>C genotype. Finally, the model was used to perform power calculations to illustrate the application of mechanistic modeling to guide the design of prospective clinical studies.

MATERIALS AND METHODS

Repaglinide Clinical Data

Mean concentration-time and individual AUC and C_{max} data were collated for the most prevalent single nucleotide polymorphism (SNP) of OATP1B1, *SLCO1B1* c.521T>C (rs4149056). For another main OATP1B1 SNP (*SLCO1B1* c.388A>G, rs2306283) information in the literature was insufficient for inclusion in the current analysis. All repaglinide concentration data were extracted from reported clinical studies using GetData Graph Digitizer 2.24. The available data consisted of mean profiles of wild type populations (TT), heterozygous (TC) and homozygous (CC) as well as populations where the *SLCO1B1* genotype was not established (hereafter referred to as MIX). The latter is anticipated to behave similar to the TT or TC populations given the large prevalence of the wild type in the Caucasian population (36) which was the ethnicity investigated in all clinical studies collated. In total, 29 mean plasma concentration-time profiles were considered in this analysis (TT, $n=9$, TC, $n=3$, CC, $n=7$ and MIX, $n=10$) with 339 concentration time points at repaglinide doses ranging from 0.25 to 2 mg. Complete data with corresponding references are listed in the Supplementary Material (Tables I and II); dose-normalized data (to a

standard dose of 0.25 mg) are presented in Supplementary Material Figure 1 and 2.

Repaglinide Empirical Model

In an initial analysis, an empirical 2-compartmental oral model with first order absorption and lag time implemented in NONMEM v.7.2 using ADVAN4 TRANS4 was found sufficient to describe the oral concentration-time profiles of repaglinide. Optimization was performed using first-order conditional estimation method with interaction (FOCE INTER) and log-transformed data. As data represent mean concentration-time profiles, inter-individual variability values (η) estimated in this case refer to between-study variability. Estimated parameters were: CL/F, k_a, V_c/F, Q/F, V_p/F, t_{lag}, and σ_{add} and between study variability on individual parameters, $\eta_{CL/F}$, η_{ka}, $\eta_{Vc/F}$, $\eta_{Vp/F}$, $\eta_{Q/F}$ and η_{tlag}. Data were investigated for the effects of OATP1B1 genotype on any of the following parameters: CL, V_c, Q and V_p.

The parameter estimates obtained using the empirical model for CL/F, k_a, V_c/F, Q/F, V_p/F, t_{lag}, and σ_{add} were 53.4±1.85 L/h, 1.92±0.127 h^{-1},11.8±1.11 L, 27.3±2.08 L/h, 35.9±1.88 L, 0.218±0.002 h and 0.0691±0.0065, respectively. The additive error on the log-transformed data approximately translates to a 6.91% proportional error on linear scale. Model was stable, as the data obtained by bootstrap analysis (n=1000) were practically identical to the NONMEM estimates. Covariates were included for all parameters apparent on F; additional covariate was considered for CL. Due to differences in bioavailability, 521CC carriers (reduced OATP1B1 activity) had 31.0±7.79% lower estimates of V_c/F, Q/F, V_p/F and 48.0±13.0% lower estimates of CL/F. As expected, the inter-individual variability was low (here inter-study variability) ranging from 10% for t_{lag} to 24% for V_p/F. Shrinkage was generally low (<20%) with the exception of k_a where shrinkage was 36%. Detailed results, including standard goodness of the fit plots, are provided in the Supplementary Material (Table III, Figs. 3, 4 and 5). The empirical model served as a reference model to the reduced PBPK model.

Repaglinide Reduced PBPK Model

A semi-mechanistic pharmacokinetic model of repaglinide was developed including central and peripheral compartment, with a mechanistic description of metabolism/transporter processes in the liver compartment (Fig. 1). The liver represented the only site of elimination for repaglinide. A total of five ordinary differential equations were implemented, 1, representing absorption site (Abs); 2, liver blood (LB); 3, liver tissue (LT); 4, central (c) and 5, peripheral compartment (p), as illustrated in Eqs. 1, 2, 3, 4 and 5. The complete code for model NONMEM implementation is provided in the Supplementary Material.

$$\frac{dA_{Abs}}{dt} = -k_a \cdot A_{Abs} \tag{1}$$

$$V_{LB} \cdot \frac{dC_{LB}}{dt} = k_a \cdot F_G \cdot A_{Abs} + Q_H \cdot (C_c - C_{LB}) + CL_{diff} \cdot SF \cdot (fu_L \cdot C_{LT} - fu_B \cdot C_{LB}) - CL_{uptake} \cdot SF \cdot fu_B \cdot C_{LB} \tag{2}$$

$$V_{LT} \cdot \frac{dC_{LT}}{dt} = CL_{diff} \cdot SF \cdot (fu_B \cdot C_{LB} - fu_L \cdot C_{LT}) + CL_{uptake} \cdot SF \cdot fu_B \cdot C_{LB} - CL_{met} \cdot SF \cdot fu_L \cdot C_{LT} \tag{3}$$

$$V_c \cdot \frac{dC_c}{dt} = Q_H \cdot (C_{LB} - C_c) + Q \cdot (C_p - C_c) \tag{4}$$

$$V_p \cdot \frac{dC_p}{dt} = Q \cdot (C_c - C_p) \tag{5}$$

where A, C, V refer to amounts (μg), concentrations (μg/L), and volumes (L), Q, CL, k_a, F_G, f_u, SF refer to inter-compartmental clearance (L/h), intrinsic clearance (L/h), absorption rate constant (h^{-1}), fraction escaping intestinal first-pass, unbound fraction and scaling factor, respectively. The indices Abs, H, L, c, LB, LT, p, B, diff and met refer to absorption, hepatic, liver, central, liver blood, liver tissue, peripheral, blood, diffusion and metabolism, respectively; SF, refers to the physiological scaling factors (i.e., hepatocellularity, microsomal recovery and liver weight, as detailed in the text below)

Within this model, a set of parameters were fixed to *in vivo* or *in vitro* parameters as shown in Fig. 1; a list of all fixed parameters is provided in Table I. All remaining parameters were estimated within NONMEM using ADVAN13 TRANS1 (numerical solution of the set of ordinary differential equations) and the first-order conditional estimation method with interaction (FOCE INTER). Metabolism of repaglinide in the liver and subsequent biliary excretion of its metabolites represent the main route of elimination considering that total urinary excretion of repaglinide was <0.1% and of repaglinide metabolites <10% of an oral dose. Repaglinide M2 was reported to be the major metabolite excreted in urine and feces accounting for 66% of the total recovered dose (37). Availability of plasma concentration-time profiles for repaglinide metabolites is currently limited; data are often presented in arbitrary units, in particular for the main CYP2C8 metabolite M4 (38,39). In addition, metabolite data in individuals associated with either OATP1B1 or CYP2C8

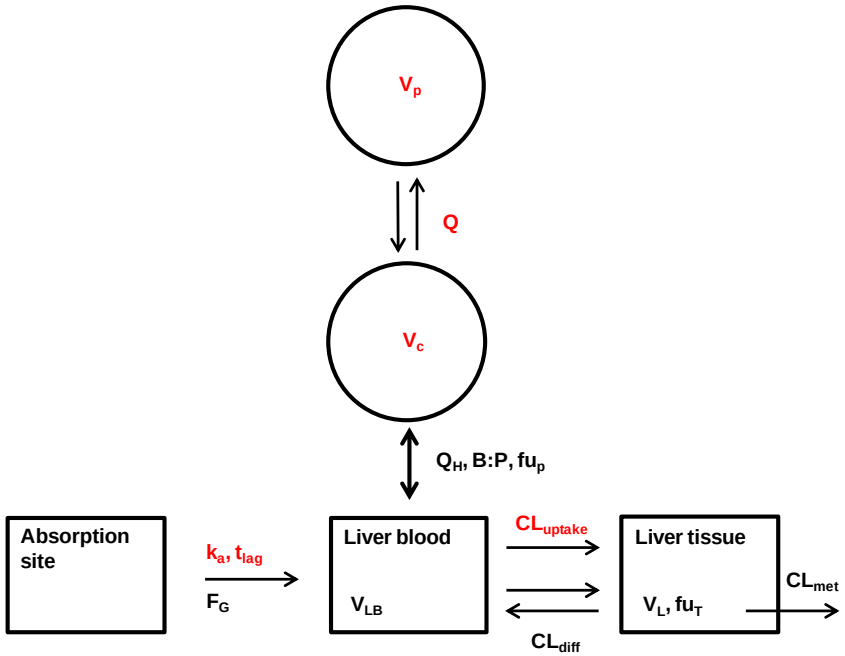

Fig. 1 Repaglinide hybrid PBPK model. The fixed parameters in the model are shown in *black*, whereas parameters estimated by the model are in *red*. Details of parameters inputs and model equations are highlighted in the Methods.

polymorphisms have not been reported and metabolites were therefore not considered in the current analysis. In addition, efflux transporters responsible for the excretion of repaglinide metabolites and any potential contribution of basolateral efflux of metabolites into blood and their distribution characteristics are currently unknown.

Previously reported repaglinide passive diffusion clearance (CL_{diff}) in plated human hepatocytes (mean value of 3 donors, (15)) was used as input parameter in the reduced model. Repaglinide metabolic clearance (CL_{met}) values reported in the literature were obtained either in human hepatocytes (27) or in human liver microsomes (40). Microsomal depletion CL_{met} was 6.8-fold higher than estimates from the hepatocytes based on the metabolite formation and this difference was reflected in the scaled CL_{met} (435 L/h *vs.* 64.2 L/h for microsomal and hepatocyte data, respectively). *In vitro-in vivo* extrapolation of the CL_{diff} and CL_{met} was performed using corresponding scaling factors, i.e., either hepatocellularity (120×10^6 cell/g liver) or microsomal recovery (40 mg/g liver). Final parameter estimates were obtained using the log-transformed data. Estimated parameters were: CL_{uptake}, k_a, V_c, Q, V_p, t_{lag}, and σ_{add} and between study variability on individual parameters: $\eta_{CLuptake}$, η_{ka}, η_{Vc}, η_{Vp}, η_Q and η_{tlag}. Bootstrap analysis was performed on $n=200$ for the reduced PBPK model. The performance of the model was assessed by visual predictive checks obtained in Matlab v.7.12 (The MathWorks® Inc.) on a number of 2,500 simulated individuals using a normal distribution of the between-study variability; random unexplained variability (σ) was included on each simulated concentration. Typical goodness of fit plots such as observations *versus* population (DV *vs.* PRED) or individual predictions (DV *vs.* IPRED) conditionally weighted residuals *versus* time (CWRES *vs.* TIME) and population predictions (CWRES *vs.* PRED) were used to detect any misspecifications in the structural model.

An identifiability analysis of the reduced PBPK model was performed using Differential Algebra for Identifiability of Systems software (DAISY) described elsewhere (41). The structural model was globally identifiable when the parameters CL_{uptake}, k_a, V_c, Q and V_p were estimated.

Table I Summary of the Parameter Values Utilized in the Semi-Mechanistic PBPK Model

Parameter	Value	Type of data	Source
V_H (L)	1.6	System	(54)
Q_H (L/h)	92.7	System	(54)
F_G	0.89	*In vivo*	(42,43)
fu_p (%)	2.6	*In vitro*	(55)
fu_T (%)	7.2	*In vitro*	(14)
B:P	0.62	*In vitro*	(55)
CL_{diff} (L/h)	129[a]	*In vitro*; plated hepatocytes ($n=3$ hepatocytes donors)	(15)
CL_{met} (L/h)	64.2[a]	*In vitro*; hepatocytes (formation, pool of 20)	(27)
	435[a]	*In vitro*; microsomes (depletion, $n=3$ pools, >100 donors)	(40)

[a] Represent the parameter values scaled using hepatocellularity or microsomal recovery

Investigation of the Effect of OATP1B1 Genotype as a Covariate

The effect of OATP1B1 genotypes on all parameters was assessed using statistical tests (one-way ANOVA tests) on the individual empirical Bayes estimates. Further, log-likelihood ratio tests at a significance level of $p<0.01$ were performed when significant differences were found on the individual estimates. No other covariates were investigated as the average age and weight were very similar across subjects in original clinical studies and additional covariate information was not reported.

Monte Carlo Simulations

In order to assess the ability of the model to recover the reported inter-individual variability of the repaglinide AUC and C_{max}, Monte Carlo simulations were performed as detailed above. A summary of the observed individual repaglinide AUC and C_{max} is provided in Table II and simulations were compared to the collated clinical observations. For the hepatic uptake clearance, true inter-individual variability was approximated from oral *in vivo* AUC data (26.2 and 35.4% for all remaining genotype groups and CC group, respectively, Table II). This approximation is correct under two assumptions: i) $CL_{diff}<<CL_{met}$ and CL_{uptake}, and ii) repaglinide oral clearance is a function of hepatic activity alone. The latter is a reasonable assumption, as the extent of intestinal metabolism is minor for repaglinide, with an average F_G of 0.89 (42,43). In the case of other parameters, between study variability obtained during the NONMEM optimization were used as surrogates for the true between subject variability. Neither Q_H nor fu_p were varied in the Monte Carlo assessment as their impact is already included in the terms V_c, V_p and CL_{uptake} for fu_p and CL_{uptake} for Q_H given the model structure.

Sensitivity Analysis

It is possible that fixing some of the model parameters may introduce a bias in the estimation of the unknown parameters and/or their variability. Certain parameters were known with fairly high confidence and fixing them has consequently introduced negligible bias. For the physiological parameters (Q_H and V_L) and the other drug related parameters (F_G, B:P, fu_p and fu_L) average values sourced from the literature were considered appropriate estimates as i) the data utilized during the optimization represented mean concentration-time profiles and ii) clinical data were obtained in a highly homogeneous population with respect to age and weight (Supplementary Material Table I). In contrast, model sensitivity on the *in vitro* parameters CL_{diff} and CL_{met} was assessed as both parameters are associated with considerable uncertainty given the experimental procedures by which they are determined and a wide range of values reported in the literature (7,15,27,40). Consequently, NONMEM optimizations were performed as detailed above by varying fixed values of CL_{met} and CL_{diff} from 0.1, 0.5, 1, 2 to 10-fold of the original value resulting in a total of 25 permutations. The estimated CL_{uptake} values in each of the scenario were compared to the reported *in vitro* value (15) and corresponding empirical scaling factors for hepatic intrinsic uptake clearance were determined as $ESF_{uptake}=CL_{uptake,in\ vivo}/CL_{uptake,\ in\ vitro}$.

Table II Individual Repaglinide AUC and C_{max} Data (Normalized to an Oral Dose of 0.25 mg) in Different SLCO1B1 Genotype Populations; Values in Parentheses Refer to the Number of Individuals

SLCO1B1 c.521T>C	AUC (ng.h/mL)	%CV	C_{max} (ng/mL)	%CV
TT	4.68 (87)[a]	25.8	3.85 (43)	30.9
TC	4.87 (12)[a]	27.6	n/a	n/a
CC	8.10 (34)	35.4	6.24 (29)	29.0
MIX	4.10 (63)[b]	56.1[b]	5.47 (20)[b]	45.4[b]

[a] Average value and %CV of TT+TC carriers are 4.75 (26.2)

[b] Inflated values and variability anticipated as population is heterogeneous

Liver Kp (liver-to-plasma concentration ratio) estimates were calculated from the AUC_∞ of the liver tissue relative to the AUC_∞ of the effluent liver plasma (44). For repaglinide, which is not excreted into the bile, the Kp_L and Kp_{uu} values at steady-state are defined by Eqs. 6 and 7, respectively.

$$Kp_L = \frac{AUC_{LT}}{AUC_{LB}/BP} = \frac{CL_{uptake} + CL_{diff}}{CL_{diff} + CL_{met}} \cdot \frac{fu_p}{fu_T} \tag{6}$$

$$Kp_{uu} = \frac{CL_{uptake} + CL_{diff}}{CL_{diff} + CL_{met}} \tag{7}$$

Impact of Parameter Uncertainty on the Prediction of DDI Risk

The uncertainty in the *in vitro* parameter estimates of CL_{met} and CL_{diff} on the CL_{uptake} optimization was further propagated into the simulation of the DDI risk. The reduced PBPK model was used to predict the fold-change in repaglinide AUC in the presence of hepatic uptake or metabolic inhibitor and the propensity of introducing a bias in the DDI assessment due to uncertainty in these parameter estimates was assessed. Cyclosporine was selected as an example of a potent inhibitor of active uptake and the magnitude of DDI was investigated using a simulated concentration-time profile of the inhibitor after 100 mg and 300 mg doses of cyclosporine Neoral® using

previously developed cyclosporine PBPK model (4). The DDI predictions were performed assuming reversible inhibition of OATP1B1 mediated uptake of repaglinide by cyclosporine and utilizing the inhibitor plasma concentration time profile to generate a dynamic change in the hepatic uptake clearance, Eq. 8. The inhibitory potency of cyclosporine $K_i = 0.019$ μM reported previously (4) was determined in HEK-OATP1B1 following a 30 min pre-incubation step. Complete inhibition of intestinal metabolism was assumed in the presence of cyclosporine, i.e., repaglinide $F_G = 1$ under these conditions; rationale supported by previous studies (4,42).

$$CL_{uptake}(t) = CL_{uptake} \cdot \left(1 + \frac{[CsA]_t}{K_i}\right) \quad (8)$$

In addition to the inhibition of active uptake, sensitivity analysis investigated the impact of parameter uncertainty on the prediction of metabolic DDI. In this analysis, complete reduction of metabolic intrinsic clearance was investigated assuming either 50% or 90% contribution of the inhibited pathway (e.g., for CYP2C8), as reported previously for repaglinide (27,38). For the metabolic interaction a constant reduction of CL_{met} was assumed, mimicking the behavior of an irreversible inhibitor. This assumption is correct when the degradation rate constant of the enzyme is << terminal elimination rate constant of repaglinide, which is appropriate, as repaglinide elimination half life in control conditions is ~1.5 h and considerably shorter than the typical degradation half life of metabolic enzymes (e.g., 23 h reported for CYP2C8, (45)). All simulations were performed in Matlab v.7.12 using the semi-mechanistic model specified in Eqs. 1–5 and the stiff ordinary differential equation solver ODE15s.

Assessment of CYP2C8 Polymorphism on Repaglinide Plasma Exposure by Simulations

In order to predict the effect of CYP2C8*3 polymorphism on repaglinide plasma exposure, the developed reduced PBPK model was used to simulate virtual individuals, as detailed in the "Monte Carlo Simulations" section. Limited evidence from both clinical (28,31) and *in vitro* (46) observations indicate that this polymorphism increases the metabolic CYP2C8 activity towards repaglinide. However, assessment of the interplay between CYP2C8 and OATP1B1 and effects of their respective SNPs has not been reported in the same individual. In order to assess the effect of combinations of these covariates, different scenarios with regards to the increase in repaglinide CL_{met} were investigated in the simulations: 1 (no increase), 1.2, 1.3, 1.5, 2, 3, 5, 10, 20 and 100-fold of the original value. In all scenarios investigated, absence of a *SLCO1B1* c.521T>C genotype that alters OATP1B1 activity (CC) was assumed. For every scenario, 1,000 individuals were simulated in order to obtain an accurate prediction of the mean AUC and the related variability. In addition, all CYP2C8*3 polymorphism scenarios outlined above were investigated in individuals with reduced OATP1B1 activity using the covariate effect identified in the model with respect to the *SLCO1B1* c.521CC genotype. Finally, the case where another CYP2C8 polymorphism or a potential DDI is decreasing rather than increasing repaglinide CL_{met} was assessed by investigating the following scenarios: 1 (no decrease in CL_{met}), 0.8, 0.7, 0.6, 0.5, 0.4, 0.3, 0.2, 0.1 and 0.05-fold of the original CL_{met} value. As above, this procedure was performed for both subjects with normal and reduced OATP1B1 activity.

Statistical Power to Identify the Effect of CYP2C8 Polymorphism or its Inhibition on Repaglinide Plasma Exposure

The reduced PBPK model was used to inform power calculations and estimate the sample size needed to identify the effects of CYP2C8*3 polymorphism on repaglinide plasma exposure. The power calculations were performed by simulation as explained below: Increasing sample sizes were evaluated, assuming that in these populations the frequency of the rare genotype that alters repaglinide AUC is 0.14 (approximate allelic frequency of CYP2C8*3 (47,48)). This fraction of the population (referring to the CYP2C8*1/*3 genotype) was simulated with the developed model using an increased value of CL_{met} and all the potential scenarios mentioned in the previous section were assessed. In order to account for the variability introduced from the *SLCO1B1* genotype, the virtual individuals in both the wild type and the variant CYP2C8 group were simulated with a 1.5% probability of being homozygous variant for the c.521T>C polymorphism (the approximate genotype CC frequency in a global population is around 0.015). A two sample *t*-test assuming equal variance and normality of the observations was performed between the plasma exposure in virtual individuals with the wild type and the variant CYP2C8 genotype. This statistical test was evaluated (5,000 times) in 5,000 simulated virtual populations of this sample size and the statistical power was calculated as the fraction of the tests in which the null hypothesis of no genotype effect was rejected ($p < 0.05$). This procedure was repeated for every sample size step. In addition, the above power calculation procedure was repeated for the case where another CYP2C8 polymorphism or a potential DDI is decreasing repaglinide CL_{met}; all the potential scenarios mentioned in the previous section were investigated, assuming in this case equal allocation of subjects between the two studied groups.

RESULTS

In the current study, 29 datasets of repaglinide clinical data reported for the most prevalent OATP1B1 polymorphism (*SLCO1B1* c.521T>C) were used in the population modeling approach to estimate repaglinide CL_{uptake} in different OATP1B1 genotype groups. Repaglinide plasma concentration-time profiles were well defined by the reduced PBPK model outlined in Fig. 1. Figure 2 illustrates the combined observed repaglinide plasma data (normalized to an oral dose of 0.25 mg) and the predicted concentration time profiles (median and 90% prediction intervals) in two genotype groups, 521TT, TC and MIX (hereafter referred to as group 1) and 521CC (group 2). The typical C_{max} and AUC values were 3.8 and 5.6 ng/mL and 4.74 and 8.66 ng.h/mL for groups 1 and 2, respectively. The individual and population fits for each of the 29 datasets used in the analysis are provided in the Supplementary Material Figure 6.

The parameter estimates obtained by the reduced repaglinide PBPK model are summarized in Table III. The typical goodness of fit plots are shown in Fig. 3; no bias was apparent in the fit with respect to time and predicted individual or population concentrations, nor was any bias observed due to the selected residual error model. The estimated repaglinide lag time (0.215 h) and absorption rate constant (1.90 h^{-1}) were consistent with the values obtained in the initial analysis by the empirical model (Supplementary Material Table III). The volume of distribution in blood was 34.2 L, equivalent to 21.9 L in plasma. Differences between the empirical and the semi-mechanistic model predictions of oral plasma concentration-time profiles were less than 3% at any given concentration when using the typical parameter values. Use of a higher microsomal CL_{met} value as a fixed parameter in the model resulted in estimated *in vivo* CL_{uptake} values corresponding to 217 and 113 μL/min/10^6 cells for SLCO1B1 genotype group 1 and 2, respectively (Table III). Depending on the OATP1B1 genotype group (normal 521TT or reduced transporter activity, 521CC), these *in vivo* estimates are 2.3- to 4.4-fold higher than the *in vitro* CL_{uptake} value reported previously in human hepatocytes (49 μL/min/10^6 cells, (15)). This discrepancy is more pronounced if a lower CL_{met} value (27) is considered as a model input, resulting in 5.5- to 10.4-fold under-estimation of CL_{uptake} for OATP1B1 genotype group 1 and 2, respectively. The genotypes of the hepatocyte donors utilized in the *in vitro* work (15) were undefined and the current analysis assumed that only OATP1B1 transporter is involved in the hepatic disposition of repaglinide.

Unlike the empirical model which identified a covariate effect of OATP1B1 genotype on F and CL (Supplementary Material Table III), the reduced PBPK model only identified an effect of the covariate on the CL_{uptake}. In the mechanistic model, the parameters V_c, Q and V_p represent the true parameter estimates as bioavailability is explicit within the model and consequently the estimated volume of distribution compared well with the observed data after i.v. administration (49). A significant difference ($p<0.01$) in CL_{uptake} was apparent for homozygous carriers of 521CC in comparison to 521TT, TC and MIX. While the sample size of TC was too small ($n=3$) to rule out genotype specific effects, no differences in repaglinide AUC values have been reported so far on an individual level for TC carriers *vs.* wild type (TT) (28). Differences in hepatic uptake clearance were considerable, with the 521CC group displaying a 48% reduction in CL_{uptake} compared to the other groups. This trend was also apparent when the empirical model was applied, with a 48% reduction in CL/F in OATP1B1 CC carriers relative to the wild type.

Monte Carlo Simulations

Figure 4 illustrates the success of the semi-mechanistic model to recover the inter-individual variability of oral repaglinide PK parameters, AUC and C_{max}, in different OATP1B1 genotype groups. Reported repaglinide AUC data were compiled from up to 87 individuals depending on the OATP1B1 genotype group. For an oral dose of 0.25 mg the average AUC of the 521TT, TC, CC and MIX populations were 4.68 ($n=87$, CV=26%), 5.27 ($n=12$, 28%), 8.10 ($n=34$, 35%) and 4.10 ($n=63$, 56%) ng.h/mL, respectively; a significant difference was apparent between the 521CC group and all others ($p<0.01$ one-way ANOVA test). In general, the semi-physiological model was successful in defining the between-subject variability assessed on AUC for TT/TC and CC: predicted AUC and %CV were 4.83 (25%) and 8.91 (35%), respectively. The model was less predictive of the between-subject variability in C_{max} (given the lack of true inter-individual variability of the parameters V_c, Q, V_p, k_a and t_{lag}): for groups 1 and 2 the predicted and observed %CV on C_{max} were 22 *vs.* 31 and 24 *vs.* 29%, respectively.

Sensitivity Analysis: Impact of Parameter Uncertainty of CL_{diff} and CL_{met} on the CL_{uptake} Estimates

CL_{met} and CL_{diff} were fixed parameters in the semi-mechanistic model; however, these parameters are associated with a large experimental uncertainty. Consequently, a sensitivity analysis was performed in which these values were varied in the range of 0.1- to 10-fold of their original values resulting in 25 possible combinations. For each set of fixed parameter values, a NONMEM optimization was performed utilizing the same dataset as detailed above. Comparison of required empirical scaling factors for CL_{uptake} (ESF_{uptake}) relative to CL_{met} and CL_{diff} used is illustrated in Fig. 5; the combination 1×:1× for CL_{met} and CL_{diff} represents the solution of the model detailed here. Based on the goodness of fit criteria, the oral repaglinide plasma concentration-time data for each

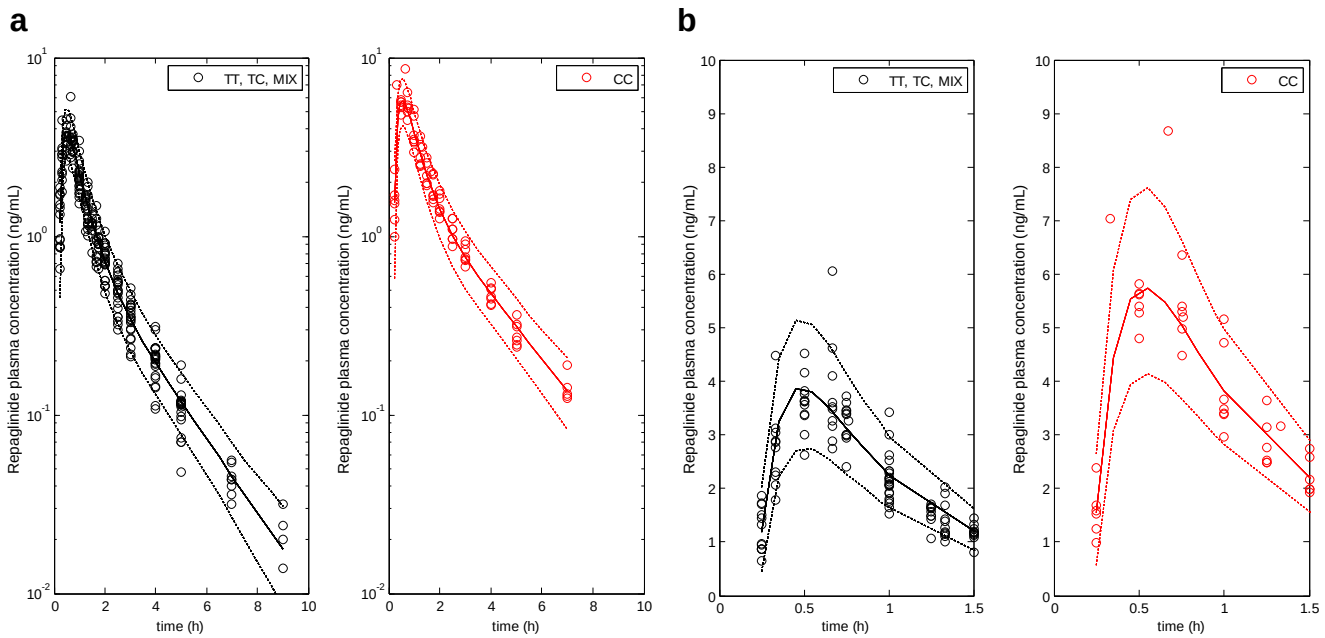

Fig. 2 (**a**) Semi-logarithmic observed and predicted plasma concentration-time profiles of repaglinide for a typical single oral dose of 0.25 mg using a reduced PBPK model stratified for OATP1B1 genotype; (**b**) shows the linear representation of the data up to 1.5 h; the *solid* and *dashed lines* represent the median and 5th and 95th percentiles of 2,500 simulations using defined parameters and between-study variability, the *open circles* represent the observed data (normalized to an oral dose of 0.25 mg).

Table III Results of the Optimization Performed in NONMEM Using Developed Reduced PBPK Model

Parameters	Mean	SE (%)
OFV	−1137.540	
$CL_{uptake,TT}$[a,b] (μL/min/10^6 cells)	217(216)	4.3
$CL_{uptake,CC}$[a,b] (μL/min/10^6 cells)	113 (114)	5.3
k_a (h^{-1})	1.90 (1.92)	7.7
V_c (L)	8.49 (8.63)	12.0
Q (L/h)	20.7 (21.0)	8.7
V_p (L)	27.3 (27.4)	4.10
t_{lag} (h)	0.215 (0.215)	1.2
σ (%)[c]	6.91 (6.84)	9.8
η_{CL} (%)	17.3 (16.8)	31.1
η_{ka} (%)	7.30 (7.10)	127
η_{Vc} (%)	15.5 (17.5)	53.1
η_{Q} (%)	22.4 (22.4)	31.9
η_{Vp} (%)	21.2 (20.8)	27.6
η_{tlag} (%)	5.86 (5.10)	47.7

Values in parenthesis and SE estimates were obtained by bootstrap analysis ($n = 250$). The V_c, Q and V_p refer to blood parameters

[a] Corresponds to CL_{uptake} values of 501 and 261 L/h for TT/TC and CC, respectively. The reference CL_{uptake} obtained *in vitro* is 49 μL/min/10^6 cells, i.e., 113 L/h (15)

[b] Use of CL_{met} reported in (27) resulted in estimated CL_{uptake} of 508 and 271 μL/min/10^6 cells for TT and CC, respectively and OFV of −1082.355. Other parameter estimates were comparable to the values listed above

[c] σ represents the additive error of the log-transformed data which approximately translates to a proportional error of the linear scale data

of the 25 combinations were equally well described (albeit not identically, as plasma C-t profiles are to some extent affected by the liver concentration as CL_{diff} represents a bidirectional process) and the objective function values were comparable (with one exception, see footnote of Table IV). It is evident that the surface of the sensitivity analysis plot is relatively flat when only a 2-fold range in CL_{met} and CL_{diff} values is considered. Within this range, the error introduced into the estimation of the uptake empirical scaling factor is reasonably small, resulting in comparable estimates of *in vivo* CL_{uptake}, as shown in Table IV. However, at the extreme cases, i.e., when either the true CL_{diff} value is 10-fold higher than the typical *in vitro* data or when the true CL_{met} value is 10-fold less than the typical *in vitro* value, the estimate of the empirical scaling factor for CL_{uptake} becomes sensitive to the values of CL_{diff} and CL_{met}. Consequently, the largest extent of underestimation of CL_{uptake} (ESF_{uptake}>50-fold) can be seen when, at the same time, the metabolic intrinsic clearance is low and the passive diffusion clearance is high (combination of 10×:0.1×). It should be noted that although the impact on repaglinide plasma concentrations is marginal across scenarios, liver concentrations are affected considerably depending on the choice of the input parameters.

Local Tissue Concentrations

The semi-mechanistic model further allowed an estimation of repaglinide accumulation ratio in the liver tissue (effective or pseudo Kp_L values) by taking into account all different

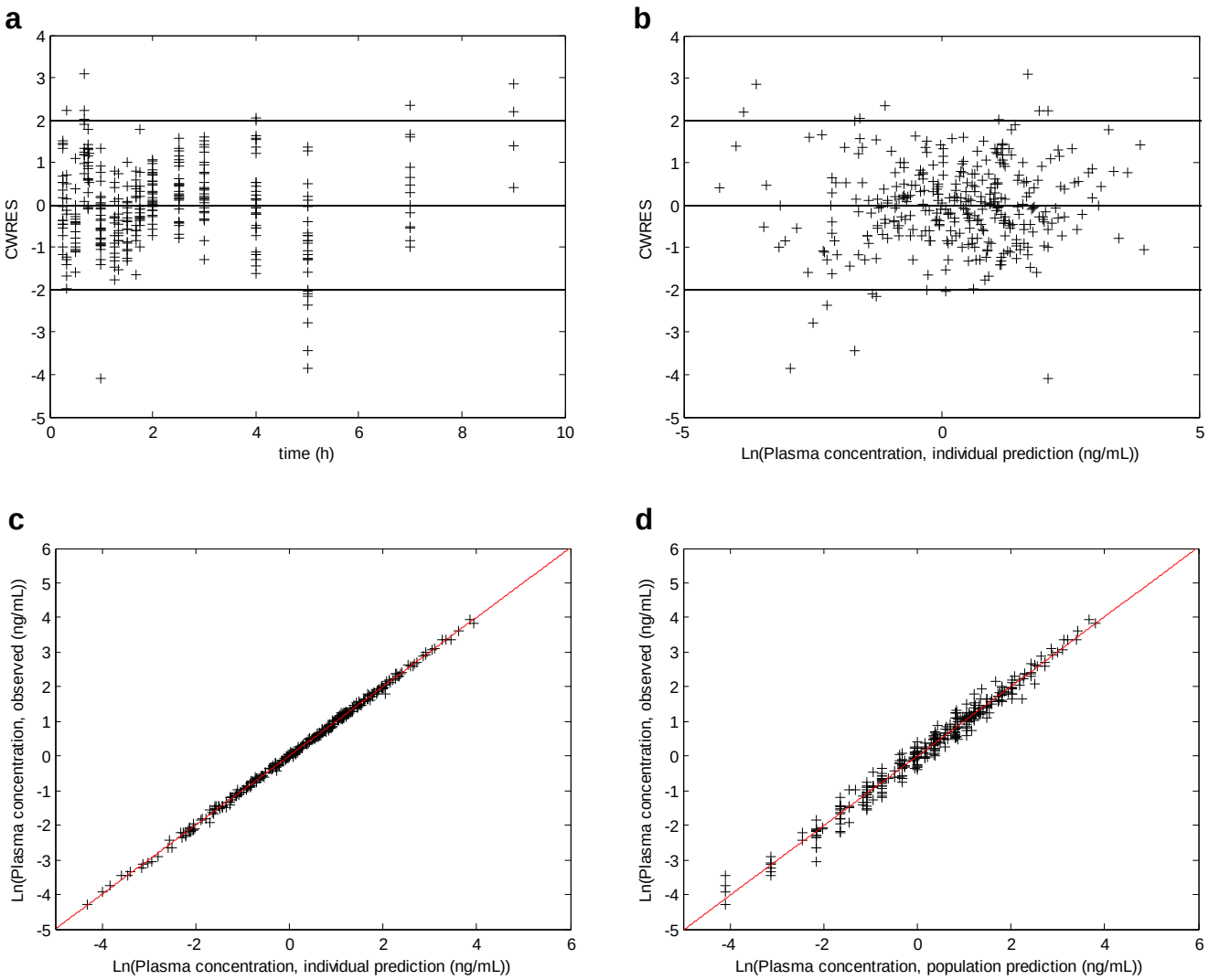

Fig. 3 Goodness of fit plots: conditionally weighted residuals (CWRES) *vs.* time (**a**) and predicted individual plasma concentration (**b**) and observed *vs.* predicted individual (**c**) and population (**d**) plasma concentration.

mechanisms. In contrast to the plasma concentration-time profiles (and AUC), the liver concentration-time profiles were highly sensitive to changes in CL_{met}, CL_{diff} and CL_{uptake}. Within the setup of the sensitivity analysis, the effective Kp_L values ranged from 0.15 to 15 (Kp_{uu}=0.42–42) depending on the combinations of CL_{met}, CL_{diff} and CL_{uptake}. The effective Kp_L values were the highest for those sets of parameter estimates where CL_{uptake} was large compared to CL_{met}; this effect was further amplified by a low CL_{diff} (see Eq. 7). For the solution of the model described here in detail (i.e., combination 1×:1× for CL_{met} and CL_{diff}) the liver AUC was 1.5-fold higher than the hepatic outlet AUC; the corresponding Kp_{uu} was 4.2.

Sensitivity Analysis: Impact of Parameter Uncertainty on DDI Predictions

The impact of utilizing different sets of fixed parameters was investigated to answer the question whether an uncertainty in the *in vitro* values of CL_{met} and CL_{diff} also propagates into the assessment of DDI risk. Simulations were performed using the solutions of the 25 cases (as shown in Fig. 5a) and the fold-change in repaglinide AUC in the presence of cyclosporine (OATP1B1 inhibitor) was investigated (Fig. 5b). Further, the impact of a constant and complete reduction of metabolic intrinsic clearance (as may be caused by an irreversible inhibitor) was investigated assuming fm_{CYP} values of the inhibited pathway of 50 and 90%. It is apparent from Fig. 5b that the change in repaglinide plasma AUC is affected to a minor degree by the final estimates of CL_{met}, CL_{diff} and CL_{uptake} when simulating the interaction with a potent OATP1B1 inhibitor (e.g., cyclosporine). Using a dose of 100 mg (CsA Neoral®) resulted in a predicted increase in the repaglinide AUC by 36 to 84% depending on the final estimates of CL_{met}, CL_{diff} and CL_{uptake}. Differences were more apparent for a 300 mg dose of CsA and 2-fold difference in the predicted effect on repaglinide AUC was evident purely because of

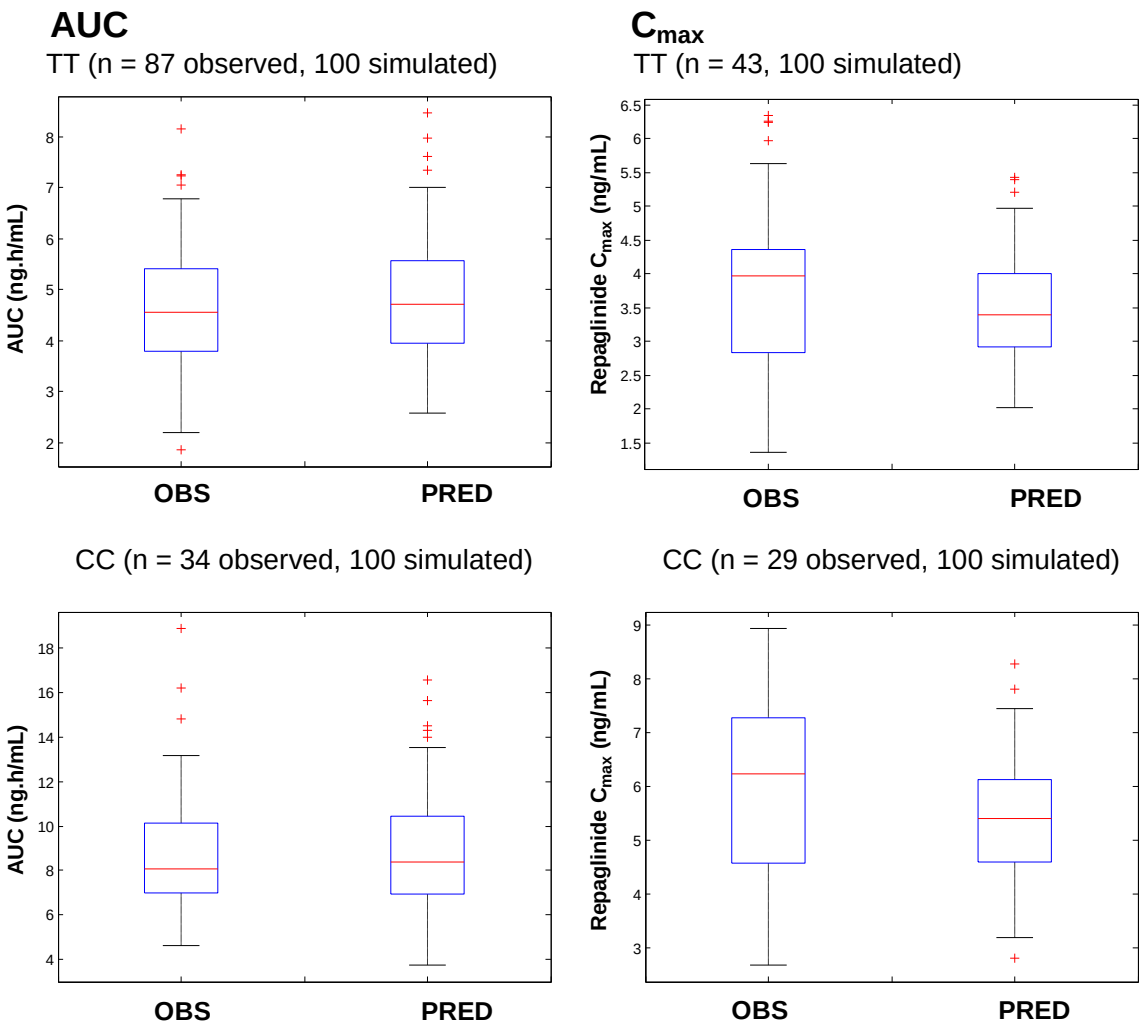

Fig. 4 Individual AUC and C_{max} values reported in the literature for TT ($n = 87$ and 43, respectively) and CC ($n = 34$ and 29, respectively) normalized to an oral repaglinide dose of 0.25 mg; predicted values are based on Monte Carlo simulations ($n = 100$) using the parameter variability specified in the methods.

different combinations of CL_{met}, CL_{diff} and CL_{uptake} (Supplementary Material Figure 7A). The worst case DDI scenario was predicted when the contribution of the passive process to the total hepatic uptake was small.

In contrast, the predicted fold-change of repaglinide plasma AUC in the presence of a metabolic inhibitor is highly affected and any predictive outcome is subject to the uncertainty in the *in vitro* parameter values of CL_{met}, CL_{diff} and CL_{uptake} (Fig. 5c). It is apparent that as CL_{diff} increases, the fold-change of AUC asymptotes the expected extent of interaction predicted by the perfusion limited considerations for liver (i.e., 10-fold increase in AUC when $fm_{CYP} = 0.90$, Supplementary Material Figure 7B). In contrast, when CL_{diff} approaches zero the fold-change in repaglinide AUC practically reduces to unity. Under these conditions, the passive diffusion is so small that the net flux of drug from the liver tissue back into plasma is insufficient to alter the plasma concentrations to any quantifiable extent. The plasma C-t profiles are completely controlled by the active uptake process (CL_{uptake}) and are consequently highly insensitive to CL_{met}. In the case of metabolic interactions, liver exposure will change to a large extent for any drug which is exclusively eliminated by this organ and for such a drug the change in liver AUC is inversely related to the reduction in metabolic intrinsic clearance.

Simulations of the Effect of CYP2C8 Polymorphism on Repaglinide Plasma Exposure

The effect of CYP2C8*3 allelic variant on repaglinide plasma exposure was simulated for a wide range of different scenarios assuming an increase in metabolic clearance in these individuals compared to the CYP2C8 wild type. This analysis was performed for individuals with normal OATP1B1 activity (Fig. 6a) and an analogous analysis for the individuals with reduced OATP1B1 activity (CC for the c.521T>C

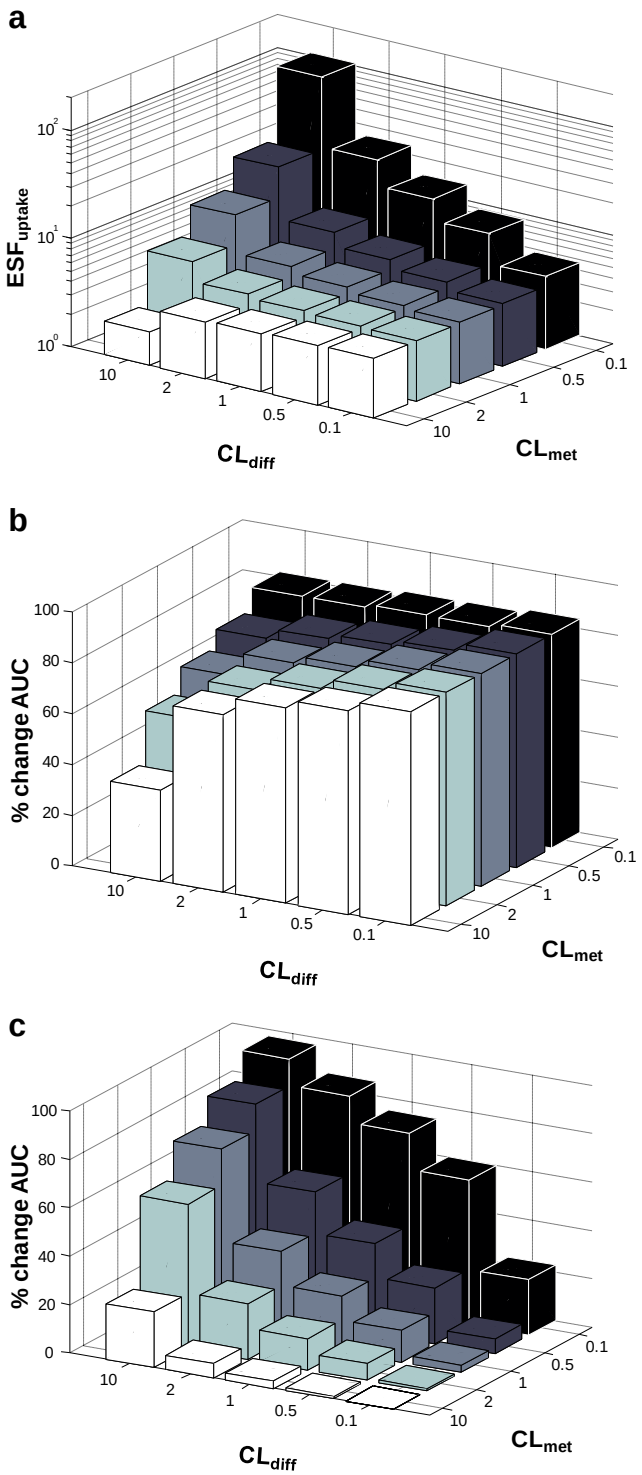

Fig. 5 (**a**) Impact of uncertainty in the *in vitro* parameters CL_{met} and CL_{diff} on the optimization of CL_{uptake} . The effect is expressed in the form of the uptake empirical scaling factor (ESF_{uptake}) required for TT population relative to the *in vitro* estimate of this parameter: $ESF_{uptake} = CL_{uptake,\ in\ vivo}/CL_{uptake,\ in\ vitro}$. (**b**) Impact of uncertainty in the *in vitro* parameters CL_{met}, CL_{diff}, and consequently CL_{uptake} on the prediction of DDI magnitude (illustrated as the % change in oral AUC) in the presence of the potent OATP1B1 inhibitor cyclosporine and (**c**) assuming irreversible metabolic inhibition and 50% contribution of the inhibited pathway to repaglinide metabolic intrinsic clearance. Assumption of the fm_{CYP} of 90% results in the same trend as shown in 5c with the difference in the magnitude of change in repaglinide AUC (see Supplementary Material Figure 7b).

polymorphism) is shown in the Supplementary Material, Figure 8. Based on the described model, the effect of the CYP2C8*3 polymorphism on repaglinide plasma exposure is predicted to be minimal. An up to 100-fold increase in CL_{met} translated to an approximate 4 to 23% change in AUC across the different scenarios investigated. In addition, AUC reaches a plateau and becomes almost completely insensitive to increase in CL_{met} beyond a 10-fold change. Analogous trends with respect to the fractional AUC decrease in the case of a CYP2C8*3 polymorphism were seen in subjects with reduced OATP1B1 activity, suggesting that the relative extent of this polymorphism effect is independent of the OATP1B1 genotype.

The opposite scenario, i.e., when another polymorphism or a potential DDI cause a decrease in repaglinide metabolic clearance is illustrated in Fig. 7a for individuals with normal OATP1B1 activity (TT). The effect on the subjects who have reduced OATP1B1 activity (CC) in addition to CYP2C8 polymorphism is shown in the Supplementary Material, Figure 9. Repaglinide AUC is insensitive (<34% increase) to moderate decreases (<60%) in repaglinide metabolic clearance. However, the effect on plasma exposure is notable with pronounced decrease in CL_{met}, e.g., a 360% increase in AUC is estimated for a 95% decrease in CL_{met}.

Power Calculations

The current analysis shows that large sample sizes are required in order to clinically detect minimal increases (<25%) in repaglinide exposure associated with the CYP2C8*3 allelic variant (Fig. 6b). It is evident that the power calculation is not only sensitive to the sample size but also to the functional effect of the polymorphism e.g., change in CYP2C8 metabolic activity. The analysis has shown that the statistical power for a given sample size is greater for the polymorphism with a larger magnitude of the effect. When the CYP2C8*3 variant increases metabolic clearance by 20% (1.2× CL_{met} scenario resulting in decrease in AUC by approximately 3.8% due to the interplay with other processes) and in order to achieve nominal 80% power, the sample size (variant genotype group) needed is >80 subjects. The equivalent sample size for the 2× CL_{met} (translates to a decrease in AUC by 11.4%) and for the 10× CL_{met} scenarios (decreases AUC by 21%) are 45 and 13 subjects, respectively.

Similar trends can be observed for the power calculations for the cases when metabolic clearance is decreased, either due to another polymorphism or a potential DDI (Fig. 7b). For the minor change in CL_{met} (20% decrease, which corresponds to 0.8× CL_{met} and a 5.6% AUC increase) sample size of >80 subjects per group is needed in order to achieve nominal 80% power. However, when the reduction in CL_{met} is more pronounced, the sample size required (per group) to detect the effect on AUC becomes much smaller.

Table IV Effect of CL_{diff} and CL_{met} on Estimated Repaglinide CL_{uptake}

Fold change in CL_{diff}	Fold change in CL_{met}									
	0.1×		0.5×		1×		2×		10×	
0.1×	**229**	*125*	**186**	*102*	**181**	*99.0*	**178**	*97.4*	**176**	*96.5*
0.5×	**432**[a]	*240*[a]	**224**	*119*	**197**	*105*	**184**	*98.0*	**173**	*92.5*
1×	**686**[a]	*382*[a]	**270**	*141*	**217**	*113*	**190**	*98.8*	**169**	*87.3*
2×	**1,190**[a]	*675*[a]	**363**	*185*	**257**	*129*	**204**	*100*	**162**	*77.2*
10×	**5,230**	*2,990*	**1,100**	*537*	**574**	*254*	**309**	*111*	**99.5**	*2.60*[b]

Values in bold represent $CL_{uptake,TT/TC}$ estimates (expressed in μL/min/10^6 cells) and values in italic estimated $CL_{uptake,CC}$

[a] Change in other parameters (k_a and V_c) observed

[b] Failure of the optimization to capture the plasma C-t profiles of repaglinide adequately

For example, sample size required for the 0.5× CL_{met} (increases AUC by 23%) and for the 0.1× CL_{met} (increases repaglinide AUC by 190%) scenarios are 27 and 3 subjects, respectively.

DISCUSSION

In the current study, a hybrid PBPK model was developed where repaglinide pharmacokinetics were defined by a mechanistic liver and empirical distribution model. The reduced or semi-mechanistic modeling approach has been successfully used previously for drugs with differential distribution properties to repaglinide, i.e., to describe nonlinear disposition of clarithromycin, as well as DDIs at the level of liver and intestine (34,50). The repaglinide model was applied to estimate hepatic active uptake clearance and assess covariate effect of *SLCO1B1* c.521T>C on its pharmacokinetics and DDI risk. All reported repaglinide clinical data, together with consideration of OATP1B1 genotype data, were included in the analysis, in contrast to previous reports that focused on data from a single study in the model development (51). The mechanistic model successfully described plasma concentration-time profiles in different OATP1B1 genotypes following oral administration of repaglinide (Fig. 2). Differences between the typical repaglinide plasma concentration time profiles obtained by the empirical 2-compartmental and the reduced PBPK model were marginal. The reduced model successfully predicted inter-individual variability in repaglinide AUC associated with different OATP1B1 genotypes (Fig. 4), whereas between-subject variability on C_{max} was under-estimated. This is not surprising due to lack of inter-individual variability information on the parameters V_c, Q, V_p, k_a and t_{lag}, as the evaluation of the

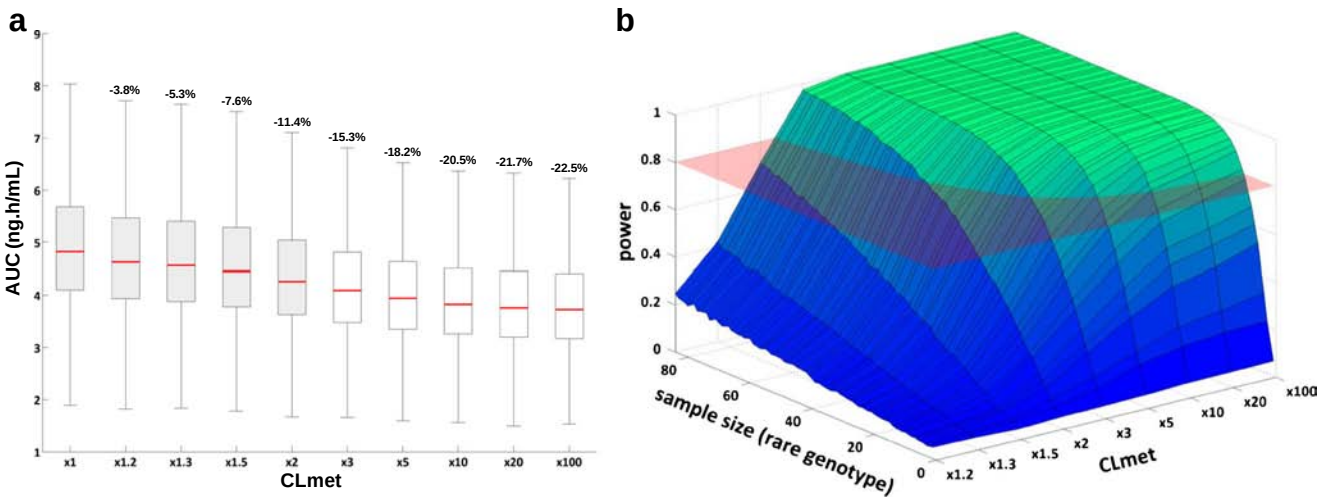

Fig. 6 (**a**) Predicted effect of CYP2C8*3 polymorphism (increase in CL_{met}) on repaglinide plasma exposure in individuals with normal OATP1B1 activity (TT/TC for the c.521T>C polymorphism). Each *boxplot* represents individual AUCs of 1,000 simulated subjects for every scenario regarding the increase in repaglinide CL_{met}. The fractional change in mean AUC relative to baseline (×1 the original value of CL_{met}) is reported. Highlighted in *grey* is the range where the increase in metabolic clearance is most probable based on *in vitro* data associated with the CYP2C8*3 variant. (**b**) Statistical power to identify the effect of CYP2C8*3 polymorphism on repaglinide plasma AUC in relation to the sample size and functional magnitude of the polymorphism effect. Sample size reported refers to the rare-variant genotype group (14% of the total study population).

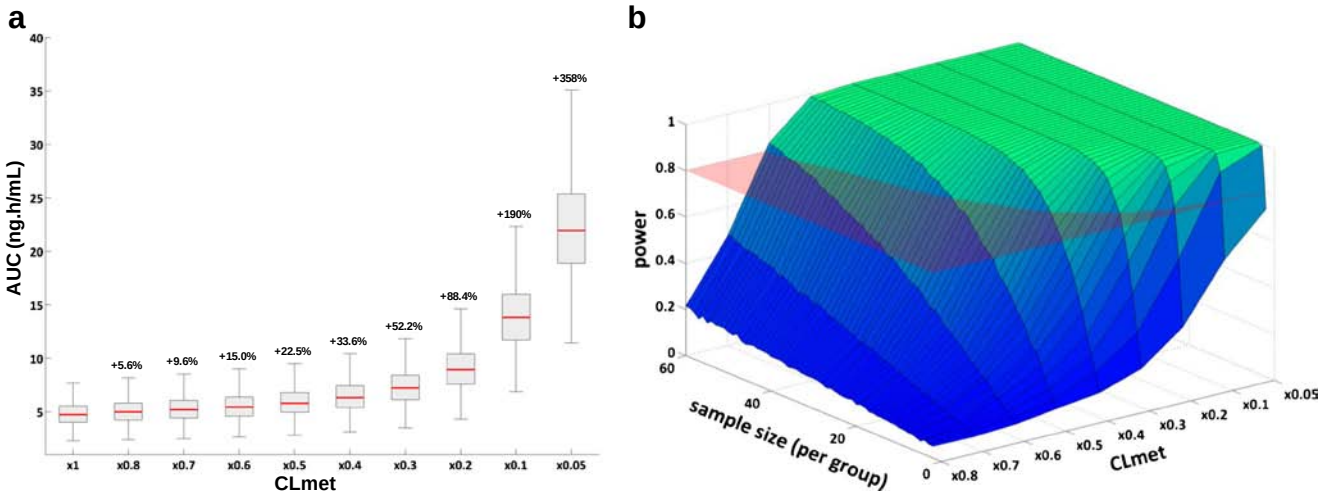

Fig. 7 (**a**) Predicted effect of either other CYP2C8 polymorphism or inhibition effect (decrease in CL_{met}) on repaglinide plasma exposure in individuals with normal OATP1B1 activity (TT/TC for the c.521T>C polymorphism). Each *boxplot* represents individual AUCs of 1,000 simulated subjects for every scenario regarding the decrease in repaglinide CL_{met} as defined in methods. The fractional change in mean AUC relative to baseline (×1 the original value of CL_{met}) is reported. (**b**) Statistical power to identify the effect of other CYP2C8 polymorphism or inhibition of CL_{met} on repaglinide plasma AUC in relation to the sample size and functional magnitude of the polymorphism/inhibition effect. Sample size is reported per group, assuming equal number of subjects in each group.

model was based on reported average plasma profiles. Ability of the model to recover the inter-individual variability in AUC allowed subsequent power calculations based on AUC and simulation of different scenarios with confidence.

The effects of *SLCO1B1* c.521T>C polymorphism on the repaglinide plasma AUC is well established (28,32) but a mechanistic PBPK model describing this behavior has not been developed previously. The current model identified a typical reduction of 48% in uptake activity for CC carriers (reduced OATP1B1 activity) relative to the other genotype groups. Although novel, the current assessment only accounted for one SNP for OATP1B1 given the available data in the literature. However, other SNPs in *SLCO1B1* gene (c.388A>G) may also be of importance in conjunction with additional SNPs of metabolizing enzymes (CYP2C8) (28). Polymorphisms of either CYP3A5 or P-gp have not been linked with any significant changes in repaglinide AUC (28), but a comprehensive covariate analysis of multiple SNPs in the same individuals is currently lacking in the literature. Another assumption made by the current model is that the hepatic active uptake of repaglinide is mediated completely by OATP1B1 which may not be the case. Emerging transporter proteomic data support this assumption, as OATP1B1 is reported as the most abundant OATP in both liver tissue and cellular *in vitro* systems (23,24). However, none of the SNPs in *SLCO1B1* gene represents a complete knock-out in repaglinide hepatic uptake; therefore, potential contribution of other transporters (e.g., OATP1B3) cannot be ruled out.

The reduced PBPK model presented here allows also prediction of DDI risk in different OATP1B1 genotype groups and assessment of the interplay between hepatic uptake and metabolism which would not be possible using a purely empirical model. However, as some elements remain empirical (e.g., volume of distribution), the extrapolative power is less than that of a full PBPK model (4,5,52). However, the current model offers a number of advantages over the full PBPK model. Unknown aspects of repaglinide distribution (e.g., uptake in other tissues) do not impact the estimates of the hepatic uptake clearance by the reduced model, as no additional predictions based on physicochemical properties are required. Currently, *in vitro* data available for repaglinide are insufficient to define with confidence uptake in any other tissues other than the liver and the frequently applied assumption that these tissues are represented by perfusion rate limited concepts may be incorrect. These shortcomings are avoided by using the modeling approach presented here. In addition, optimization process is less biased compared to full PBPK models (with typically large number of fixed parameters), facilitating Monte Carlo simulations and power analyses.

The hybrid model also highlights the considerable impact of CL_{diff} and CL_{met} on our ability to assess confidently CL_{uptake} from clinical data and provides additional understanding of the extensive variability in CL_{uptake} empirical scaling factors reported for the comparable set of drugs (7,15). It is important to appreciate the limited power of plasma concentration-time profiles for the parameter optimization, in particular for drugs with multiple and sequential disposition processes, as discussed recently in more detail (26). The analysis performed here has illustrated that multiple solutions can describe repaglinide plasma concentration-time profiles almost equally well, conditional on different values used for the fixed parameters (Fig. 5). To overcome the reliance on fixed parameters, a Bayesian framework has been proposed where priors are provided for the parameters

(instead of using the fixed value), allowing them to be updated with the observed clinical data, resulting in a statistical distribution of the output parameters, rather than just a single estimate. The limitation of the approach is that in some cases appropriate statistical distribution of priors might not be available. In addition, if clinical data are not as informative to update model parameters then these will shrink towards prior information (as if a fixed value was used) (26).

The uncertainties described above translate further into the predicted magnitude of DDI (Fig. 5b and c) and may affect the success of these predictions considerably, as illustrated in the example of repaglinide metabolic DDIs. Given the uncertainty in essential drug parameters CL_{diff} and even the widely studied CL_{met} by current *in vitro* methodologies, it is highly advisable to investigate a certain space of drug properties rather than a single set of parameter values in order to obtain a clearer understanding of the potential risk of DDI of a victim drug in question. It is evident from Fig. 5 that under certain conditions no DDI would have been predicted for repaglinide metabolic interaction, while other sets of parameter values suggest substantial sensitivities to metabolic inhibitors. For any other drugs analogous to repaglinide, this becomes a complex, multi-factorial problem, to be addressed within the PBPK modeling framework.

To date, clinical studies are contradictory on the overall effect of CYP2C8*3 polymorphism on repaglinide plasma exposure. Recently, this genetic variant was reported to increase repaglinide CYP2C8-mediated CL_{met} *in vitro* by approximately 30% (46). However, direct translation of this finding to an *in vivo* situation is difficult. Using the reduced PBPK model we were able to mechanistically predict minimal impact of the CYP2C8*3 polymorphism on repaglinide plasma exposure (Fig. 6a); these simulations are in agreement with the reported clinical studies where this effect ranges from none to a 48% decrease in AUC. However, it should be clearly noted that our predictions with regard to the effect of CYP2C8*3 polymorphism are conditional on the *in vitro* CL_{met} and CL_{diff} values used to inform model parameters in a similar way that their uncertainty affected the DDI assessment (Fig. 5). The analysis has also illustrated that repaglinide plasma exposure is relatively insensitive to increases in metabolic activity. From a mechanistic point of view this is justifiable, as the overall hepatic clearance and subsequently plasma exposure for drugs like repaglinide are resultant of the interplay of multiple processes. If the passive diffusion is small relative to the CL_{met} (as seen here), the dominant process for the overall clearance and plasma exposure is the hepatic uptake and not the metabolism. This is clearly illustrated for scenarios where CL_{met} is increased >10-fold, yet plasma exposure is insensitive to these changes; however, repaglinide liver exposure will be affected. When a CYP2C8 polymorphism or a potential DDI is decreasing repaglinide CL_{met} (in particular if this change is >60%) the balance between passive diffusion and CL_{met} is altered and the passive diffusion efflux process becomes governing, leading to changes in repaglinide plasma exposure.

In addition to the prediction of different scenarios (DDI and genetic polymorphisms), the current work provides an example of the application of mechanistic modeling for optimal design of a clinical study for drugs with complex pharmacokinetics affected by multiple polymorphisms. The reduced PBPK model allowed us to simulate the impact of the CYP2C8*3 polymorphism on repaglinide AUC in relation to the *SLCO1B1* c.521T>C genotype, overcoming the sample size difficulties that will be associated with such an investigation in a clinical setting. The relative effect of the CYP2C8*3 polymorphism was shown to be independent of the OATP1B1 genotype, as the fractional AUC changes in individuals with normal and decreased OATP1B1 activity were equivalent (Fig. 6 and Supplementary Material Figure 8). The findings of this work have direct implications for the design of pharmacogenetic studies. The basis of an adequate power calculation prior to a pharmacogenetic study is an educated guess on the magnitude of the polymorphism effect on the observed outcome and the associated variability (53). Repaglinide represents an example of a drug where the magnitude of the functional effect of a polymorphism (e.g., increase in metabolic activity) is not directly reflected in the observed clinical output i.e., plasma exposure. In such a case, *in vitro* information on the magnitude of the polymorphic effect cannot directly inform the design of a pharmacogenetic study and rationalise the required study size without the use of mechanistic modeling. Current repaglinide PBPK model adequately captures not only the mean repaglinide plasma exposure but also the associated population variability, allowing us to perform power calculations for different magnitudes of functional effect of CYP2C8 polymorphism. These power calculations indicate that large sample sizes will be needed to clinically detect the effect of this polymorphism and minimal changes in repaglinide plasma exposure. Additional power calculations performed for the more common scenario where CYP2C8 metabolic clearance is decreased (additional polymorphism or inhibition) can be used to guide future pharmacogenetic and/or DDI studies.

In conclusion, the hybrid PBPK model represents a valuable tool for parameter optimization and assessment of covariate effects compared to the whole body PBPK model. Limitations of parameter estimation based solely on plasma data as a surrogate for tissue profiles are highlighted. The mechanistic model-based approach presented here has additional advantages as it provides a framework to inform power calculation and design of either pharmacogenetic or DDI studies even in the first stages of drug development when the information about the effects of a genetic variant or enzyme inhibition *in vivo* are likely to be limited.

ACKNOWLEDGMENTS AND DISCLOSURES

The work was funded by a consortium of pharmaceutical companies within the Centre for Applied Pharmacokinetic Research, University of Manchester (http://www.pharmacy.manchester.ac.uk/capkr/).

NT is a recipient of a PhD studentship from University of Manchester and Eli Lilly and Company, Indianapolis, USA.

REFERENCES

1. Jones H, Rowland-Yeo K. Basic concepts in physiologically based pharmacokinetic modeling in drug discovery and development. CPT Pharmacometrics Syst Pharmacol. 2013;2:e63.
2. Rostami-Hodjegan A. Physiologically based pharmacokinetics joined with in vitro-in vivo extrapolation of adme: a marriage under the arch of systems pharmacology. Clin Pharmacol Ther. 2012;92:50–61.
3. Gertz M, Houston JB, Galetin A. Physiologically based pharmacokinetic modeling of intestinal first-pass metabolism of CYP3A substrates with high intestinal extraction. Drug Metab Dispos. 2011;39:1633–42.
4. Gertz M, Cartwright CM, Hobbs MJ, Kenworthy KE, Rowland M, Houston JB, *et al.* Application of PBPK modeling in the assessment of the interaction potential of cyclosporine against hepatic and intestinal uptake and efflux transporters and CYP3A4. Pharm Res. 2013;30:761–80.
5. Varma MV, Lai Y, Kimoto E, Goosen TC, El-Kattan AF, Kumar V. Mechanistic modeling to predict the transporter- and enzyme-mediated drug-drug interactions of repaglinide. Pharm Res. 2013;30:1188–99.
6. Zamek-Gliszczynski MJ, Lee CA, Poirier A, Bentz J, Chu X, Ishikawa T, *et al.* ITC recommendations on transporter kinetic parameter estimation and translational modeling of transport-mediated PK and DDIs in humans. Clin Pharmacol Ther. 2013;94(1):64–79.
7. Jones HM, Barton HA, Lai Y, Bi YA, Kimoto E, Kempshall S, *et al.* Mechanistic pharmacokinetic modeling for the prediction of transporter-mediated disposition in humans from sandwich culture human hepatocyte data. Drug Metab Dispos. 2012;40:1007–17.
8. Poirier A, Funk C, Scherrmann JM, Lave T. Mechanistic modeling of hepatic transport from cells to whole body: application to napsagatran and fexofenadine. Mol Pharm. 2009;6:1716–33.
9. Watanabe T, Kusuhara H, Maeda K, Shitara Y, Sugiyama Y. Physiologically based pharmacokinetic modeling to predict transporter-mediated clearance and distribution of pravastatin in humans. J Pharmacol Exp Ther. 2009;328:652–62.
10. Kusuhara H, Sugiyama Y. Pharmacokinetic modeling of the hepatobiliary transport mediated by cooperation of uptake and efflux transporters. Drug Metab Rev. 2010;42:539–50.
11. Shitara Y, Maeda K, Ikejiri K, Yoshida K, Horie T, Sugiyama Y. Clinical significance of organic anion transporting polypeptides (OATPs) in drug disposition: their roles in hepatic clearance and intestinal absorption. Biopharm Drug Dispos. 2013;34:45–78.
12. Poirier A, Lave T, Portmann R, Brun ME, Senner F, Kansy M, *et al.* Design, data analysis, and simulation of in vitro drug transport kinetic experiments using a mechanistic in vitro model. Drug Metab Dispos. 2008;36:2434–44.
13. Paine SW, Parker AJ, Gardiner P, Webborn PJ, Riley RJ. Prediction of the pharmacokinetics of atorvastatin, cerivastatin, and indomethacin using kinetic models applied to isolated rat hepatocytes. Drug Metab Dispos. 2008;36:1365–74.
14. Menochet K, Kenworthy KE, Houston JB, Galetin A. Simultaneous assessment of uptake and metabolism in rat hepatocytes: a comprehensive mechanistic model. J Pharmacol Exp Ther. 2012;341:2–15.
15. Menochet K, Kenworthy KE, Houston JB, Galetin A. Use of mechanistic modelling to assess inter-individual variability and interspecies differences in active uptake in human and rat hepatocytes. Drug Metab Dispos. 2012;40:1744–56.
16. Lee JK, Marion TL, Abe K, Lim C, Pollock GM, Brouwer KL. Hepatobiliary disposition of troglitazone and metabolites in rat and human sandwich-cultured hepatocytes: use of Monte Carlo simulations to assess the impact of changes in biliary excretion on troglitazone sulfate accumulation. J Pharmacol Exp Ther. 2010;332:26–34.
17. Yabe Y, Galetin A, Houston JB. Kinetic characterization of rat hepatic uptake of 16 actively transported drugs. Drug Metab Dispos. 2011;39:1808–14.
18. Nordell P, Winiwarter S, Hilgendorf C. Resolving the distribution-metabolism interplay of eight OATP substrates in the standard clearance assay with suspended human cryopreserved hepatocytes. Mol Pharm. 2013;10:4443–51.
19. Camenisch G, Umehara K. Predicting human hepatic clearance from in vitro drug metabolism and transport data: a scientific and pharmaceutical perspective for assessing drug-drug interactions. Biopharm Drug Dispos. 2012;33:179–94.
20. Hallifax D, Foster JA, Houston JB. Prediction of human metabolic clearance from in vitro systems: retrospective analysis and prospective view. Pharm Res. 2010;27:2150–61.
21. Badolo L, Rasmussen LM, Hansen HR, Sveigaard C. Screening of OATP1B1/3 and OCT1 inhibitors in cryopreserved hepatocytes in suspension. Eur J Pharm Sci. 2011;40:282–8.
22. Ulvestad M, Bjorquist P, Molden E, Asberg A, Andersson TB. OATP1B1/1B3 activity in plated primary human hepatocytes over time in culture. Biochem Pharmacol. 2011;82:1219–26.
23. Kimoto E, Yoshida K, Balogh LM, Bi YA, Maeda K, El-Kattan A, *et al.* Characterization of organic anion transporting polypeptide (OATP) expression and its functional contribution to the uptake of substrates in human hepatocytes. Mol Pharm. 2012;9:3535–42.
24. Ohtsuki S, Schaefer O, Kawakami H, Inoue T, Liehner S, Saito A, *et al.* Simultaneous absolute protein quantification of transporters, cytochromes P450, and UDP-glucuronosyltransferases as a novel approach for the characterization of individual human liver: comparison with mRNA levels and activities. Drug Metab Dispos. 2012;40:83–92.
25. van de Steeg E, Greupink R, Schreurs M, Nooijen IH, Verhoeckx KC, Hanemaaijer R, *et al.* Drug-drug interactions between rosuvastatin and oral antidiabetic drugs occurring at the level of OATP1B1. Drug Metab Dispos. 2013;41:592–601.
26. Tsamandouras N, Rostami-Hodjegan A, Aarons L. Combining the "bottom-up" and "top-down" approaches in pharmacokinetic modelling: Fitting PBPK models to observed clinical data. Br J Clin Pharmacol. 2013.
27. Sall C, Houston JB, Galetin A. A comprehensive assessment of repaglinide metabolic pathways: impact of choice of in vitro system and relative enzyme contribution to in vitro clearance. Drug Metab Dispos. 2012;40:1279–89.
28. Niemi M, Backman JT, Kajosaari LI, Leathart JB, Neuvonen M, Daly AK, *et al.* Polymorphic organic anion transporting polypeptide 1B1 is a major determinant of repaglinide pharmacokinetics. Clin Pharmacol Ther. 2005;77:468–78.
29. Bidstrup TB, Damkier P, Olsen AK, Ekblom M, Karlsson A, Brosen K. The impact of CYP2C8 polymorphism and grapefruit juice on the pharmacokinetics of repaglinide. Br J Clin Pharmacol. 2006;61:49–57.

30. Tomalik-Scharte D, Fuhr U, Hellmich M, Frank D, Doroshyenko O, Jetter A, *et al.* Effect of the CYP2C8 genotype on the pharmacokinetics and pharmacodynamics of repaglinide. Drug Metab Dispos. 2011;39:927–32.
31. Niemi M, Leathart JB, Neuvonen M, Backman JT, Daly AK, Neuvonen PJ. Polymorphism in CYP2C8 is associated with reduced plasma concentrations of repaglinide. Clin Pharmacol Ther. 2003;74:380–7.
32. Kalliokoski A, Neuvonen M, Neuvonen PJ, Niemi M. The effect of SLCO1B1 polymorphism on repaglinide pharmacokinetics persists over a wide dose range. Br J Clin Pharmacol. 2008;66:818–25.
33. Quinney SK, Zhang X, Lucksiri A, Gorski JC, Li L, Hall SD. Physiologically based pharmacokinetic model of mechanism-based inhibition of CYP3A by clarithromycin. Drug Metab Dispos. 2010;38:241–8.
34. Ito K, Ogihara K, Kanamitsu S, Itoh T. Prediction of the in vivo interaction between midazolam and macrolides based on in vitro studies using human liver microsomes. Drug Metab Dispos. 2003;31:945–54.
35. Cao Y, Jusko WJ. Applications of minimal physiologically-based pharmacokinetic models. J Pharmacokinet Pharmacodyn. 2012;39:711–23.
36. Niemi M, Pasanen MK, Neuvonen PJ. Organic anion transporting polypeptide 1B1: a genetically polymorphic transporter of major importance for hepatic drug uptake. Pharmacol Rev. 2011;63:157–81.
37. van Heiningen PN, Hatorp V, Kramer Nielsen K, Hansen KT, van Lier JJ, De Merbel NC, *et al.* Absorption, metabolism and excretion of a single oral dose of (14)C-repaglinide during repaglinide multiple dosing. Eur J Clin Pharmacol. 1999;55:521–5.
38. Honkalammi J, Niemi M, Neuvonen PJ, Backman JT. Dose-dependent interaction between gemfibrozil and repaglinide in humans: strong inhibition of CYP2C8 with subtherapeutic gemfibrozil doses. Drug Metab Dispos. 2011;39:1977–86.
39. Tornio A, Niemi M, Neuvonen M, Laitila J, Kalliokoski A, Neuvonen PJ, *et al.* The effect of gemfibrozil on repaglinide pharmacokinetics persists for at least 12 h after the dose: evidence for mechanism-based inhibition of CYP2C8 in vivo. Clin Pharmacol Ther. 2008;84:403–11.
40. Gertz M, Harrison A, Houston JB, Galetin A. Prediction of human intestinal first-pass metabolism of 25 CYP3A substrates from in vitro clearance and permeability data. Drug Metab Dispos. 2010;38:1147–58.
41. Bellu G, Saccomani MP, Audoly S, D'Angio L. DAISY: a new software tool to test global identifiability of biological and physiological systems. Comput Methods Prog Biomed. 2007;88:52–61.
42. Gertz M, Davis JD, Harrison A, Houston JB, Galetin A. Grapefruit juice-drug interaction studies as a method to assess the extent of intestinal availability: utility and limitations. Curr Drug Metab. 2008;9:785–95.
43. Bidstrup TB, Bjornsdottir I, Sidelmann UG, Thomsen MS, Hansen KT. CYP2C8 and CYP3A4 are the principal enzymes involved in the human in vitro biotransformation of the insulin secretagogue repaglinide. Br J Clin Pharmacol. 2003;56:305–14.
44. Gallo JM, Lam FC, Perrier DG. Area method for the estimation of partition coefficients for physiological pharmacokinetic models. J Pharmacokinet Biopharm. 1987;15:271–80.
45. Backman JT, Honkalammi J, Neuvonen M, Kurkinen KJ, Tornio A, Niemi M, *et al.* CYP2C8 activity recovers within 96 hours after gemfibrozil dosing: estimation of CYP2C8 half-life using repaglinide as an in vivo probe. Drug Metab Dispos. 2009;37:2359–66.
46. Yu L, Shi D, Ma L, Zhou Q, Zeng S. Influence of CYP2C8 polymorphisms on the hydroxylation metabolism of paclitaxel, repaglinide and ibuprofen enantiomers in vitro. Biopharm Drug Dispos. 2013;34:278–87.
47. Bahadur N, Leathart JB, Mutch E, Steimel-Crespi D, Dunn SA, Gilissen R, *et al.* CYP2C8 polymorphisms in Caucasians and their relationship with paclitaxel 6alpha-hydroxylase activity in human liver microsomes. Biochem Pharmacol. 2002;64:1579–89.
48. Dai D, Zeldin DC, Blaisdell JA, Chanas B, Coulter SJ, Ghanayem BI, *et al.* Polymorphisms in human CYP2C8 decrease metabolism of the anticancer drug paclitaxel and arachidonic acid. Pharmacogenetics. 2001;11:597–607.
49. Hatorp V, Oliver S, Su CA. Bioavailability of repaglinide, a novel antidiabetic agent, administered orally in tablet or solution form or intravenously in healthy male volunteers. Int J Clin Pharmacol Ther. 1998;36:636–41.
50. Quinney SK, Galinsky RE, Jiyamapa-Serna VA, Chen Y, Hamman MA, Hall SD, *et al.* Hydroxyitraconazole, formed during intestinal first-pass metabolism of itraconazole, controls the time course of hepatic CYP3A inhibition and the bioavailability of itraconazole in rats. Drug Metab Dispos. 2008;36:1097–101.
51. Kudo T, Hisaka A, Sugiyama Y, Ito K. Analysis of the repaglinide concentration increase produced by gemfibrozil and itraconazole based on the inhibition of the hepatic uptake transporter and metabolic enzymes. Drug Metab Dispos. 2013;41:362–71.
52. Varma MV, Lin J, Bi YA, Rotter CJ, Fahmi OA, Lam JL, *et al.* Quantitative prediction of repaglinide-rifampicin complex drug interactions using dynamic and static mechanistic models: delineating differential CYP3A4 induction and OATP1B1 inhibition potential of rifampicin. Drug Metab Dispos. 2013;41:966–74.
53. Williams JA, Johnson K, Paulauskis J, Cook J. So many studies, too few subjects: establishing functional relevance of genetic polymorphisms on pharmacokinetics. J Clin Pharmacol. 2006;46:258–64.
54. International Commission on Radiological Protection. Basic anatomical and physiological data for use in radiological protection: reference values. A report of age- and gender-related differences in the anatomical and physiological characteristics of reference individuals. ICRP Publication 89. Ann ICRP. 2002;32:5–265.
55. Hatorp V, Walther KH, Christensen MS, Haug-Pihale G. Single-dose pharmacokinetics of repaglinide in subjects with chronic liver disease. J Clin Pharmacol. 2000;40:142–52.